The American Mineralogist, Volume 60, pages 854–862, 1975

Physical Properties of Some Synthetic Fe-Mg-Al Trioctahedral Biotites

DAVID A. HEWITT

Department of Geological Sciences,
Virginia Polytechnic Institute and State University, Blacksburg, Virginia 24061

AND DAVID R. WONES

U.S. Geological Survey, National Center 959
Reston, Virginia 22092

Abstract

Twenty-nine biotities corresponding to the formula $K(Mg_xFe_yAl_z)Al_{1+z}Si_{3-z}O_{10}(OH)_2$, where $z = 3\text{-}x\text{-}y$, have been crystallized hydrothermally from oxide mixes. Syntheses were carried out at $P_{fluid} = 1000$ bars, $P_{H_2} = 100$ bars, and $T = 700°–770°C$ for the Fe-bearing biotites, and at $P_{H_2O} = 1000–2000$ bars and $T = 800°–850°C$ for the Fe-free biotites. Multiple regression analyses of the unit cell parameters for $1M$ micas and of the optical indices of the refraction yield:

$$a(\text{Å}) = 5.406(1) - 0.089(2)\frac{x}{x+y} - 0.056(3)z + 0.022(4)\frac{zx}{x+y} \quad \text{esd} = 0.002$$

$$n\gamma = 1.686(1) - 0.103(2)\frac{x}{x+y} - 0.029(3)z + 0.037(4)\frac{zx}{x+y} \quad \text{esd} = 0.001$$

$$\text{where} \quad 0 \leq \frac{x}{x+y} \leq 1 \quad \text{and} \quad 0 \leq z \leq 0.75 \pm 0.1$$

Calculations of the α-tetrahedral rotation angle and the K–O bond length on the basis of an ideal trioctahedral mica show that for the most aluminous biotites the α rotations range from 12° to 14.7°, corresponding to K–O bond lengths of 2.89 to 2.77 Å respectively. If the smaller Na^+ or Ca^{2+} ion is substituted for the K^+ ion, the amount of Al substitution and the amount of α rotation can be increased substantially. These data suggest that an important structural factor limiting the trioctahedral Al-substitution is the decreasing size of the interlayer site resulting from increased tetrahedral rotation.

Biotites synthesized at $T > 700°C$ appear to be $1M$ or $3T$ polytypes. At lower temperatures, the Mg-biotites showed increasing amounts of what appears to be a $2M_1$ polytype in a $1M$–$2M_1$ mixture; thus, if the $2M_1$ polytype has a stability field, it probably lies at relatively low temperatures.

Although the substitutions $Fe^{2+} \rightleftarrows Mg^{2+}$ and $Mg^{2+} + Si^{4+} \rightleftarrows 2Al^{3+}$ occur with essentially zero volume of mixing, the substitution $Fe^{2+} + Si^{4+} \rightleftarrows 2Al^{3+}$ has a net positive volume of mixing. This indicates that the solution properties of the Fe-Al biotites are not ideal and suggests that there could be octahedral ordering in the Fe-Al-rich biotites.

Introduction

The determination and understanding of the solid-solution limits and the physical properties of the trioctahedral biotites containing Mg, Fe, and Al in the octahedral sites are necessary in order to carry out experimental investigations such as the Fe-Mg-Al distributions between biotites and other ferromagnesian minerals. For the assemblages of fine-grained mineral aggregates generally encountered in experimental run products, optical and X-ray analysis remain the most practical methods for the determination of coexisting phase compositions. Eugster *et al* (1972) recently used the electron microprobe in a study of the muscovite-paragonite system, but the procedures are not routine.

Previous studies on biotite solid solutions involving Mg, Fe, and Al substitution in the octahedral sites are available for the Mg-Al biotites (Crowley and Roy, 1964; Hazen and Wones, 1972; Yoder and Eugster, 1954), the Fe-Al biotites (Rutherford, 1973), and the Fe-Mg biotites (Wones, 1963); however, no data are yet available on the mixed substitution of Fe, Mg, and Al.

Wones (1963) and Rutherford (1973) have shown that the cell parameters and indices of refraction of the synthetic iron-bearing biotites vary as a function of composition and the hydrogen fugacity present during formation. Because of the large number of runs necessary to determine the variation of physical properties in the Mg-Fe-Al biotites for even one given pressure of hydrogen, the data were collected only for biotites synthesized at 100 bars hydrogen pressure and 1000 bars total pressure. Under these conditions, the Fe^{3+} content of the biotites will generally be low, but can reach as much as 10 percent for the iron-rich biotites (Wones, Burns, and Carroll, 1971; Hazen and Wones, 1972). The need for additional data at other hydrogen fugacities is obvious.

Experimental Procedures

All the biotites used in this investigation were synthesized directly from oxide mixes at hydrogen pressures, total pressures, and temperatures indicated in Table 1. The biotite compositions synthesized are shown in Figure 1.

Oxide mixes for the phases were prepared from reagent-grade materials. K_2O and SiO_2 were added as $K_2Si_4O_9$ or $K_2Si_6O_{13}$ glass prepared using the technique of Schairer and Bowen (1955). Additional silica glass (Corning Lump Cullet #7940) was added to the mixture when the K/Si ratios varied from either 1:2 or 1:3. Magnesium was added in the form of MgO fired at 1200°C; iron was added as Fe_2O_3 fired at 1200°C; aluminum was added as γ-alumina prepared from $AlCl_3 \cdot 6H_2O$ by heating to constant weight at 700°C and then firing at 900°C for 1–2 hours. The materials were weighed in proportions corresponding to the formula $K(Mg_xFe_yAl_z)Al_{1+z}Si_{3-z}O_{11+y/2}$ where $z = 3\text{-}x\text{-}y$. The mixes were then ground by hand under acetone in an agate mortar for approximately 1/2 hour. Those containing iron-bearing oxides were reduced in pure hydrogen at 1 atmosphere and 600°C for approximately 1/2 hour, at which time all the iron was present as iron metal.

The iron-free biotites were synthesized hydrothermally using sealed platinum capsules in Tuttle cold-seal bombs at pressures and temperatures in the range 1000–2000 bars and 800°–850°C, respectively. All runs contained an excess of pure water over the stoichiometric amount necessary for the biotite. Iron-bearing biotites were synthesized in Shaw (1963) hydrogen diffusion bombs using hydrogen-argon mixtures as the pressure medium. All of these runs were made at 1000 bars total pressure, 100 bars hydrogen pressure, and approximately 750°C in sealed $Ag_{80}Pd_{20}$ capsules containing the reduced oxide mix and an excess of water.

Temperatures were measured using calibrated chromel-alumel thermocouples and are accurate to ±5°C. Pressures were measured with Heise Bourdon Tube gauges. Total pressures are presumed accurate to ±50 bars and hydrogen pressures accurate to ±5 bars. Run times range from 3 to 22 days. At the end of each run, the capsules were weighed and the contents removed. Only runs that retained water were acceptable. The products were then examined optically, and any run that did not contain greater than 95 percent biotite (by visual estimate) or that showed in-

TABLE 1. Run Data

Run #	z*	$\frac{x}{x+y}$ **	P_{Kbar}	P_{H_2}*** (bars)	T°C***	Duration
196-70	0	1.0	1.0	B	850	7d
222-69	0	1.0	2.0	B	700	22d
45-73	0	0.75	1.0	100	749	9d
40-73	0	0.67	1.0	100	753	6d
53-73	0	0.50	1.0	100	749	8d
68-73	0	0.25	1.0	100	747	8d
142-70	0	0.0	1.0	100	770	13d
67-73	.125	0.0	1.0	100	747	8d
55-73	.167	1.0	1.0	100	750	9d
189-70	.25	1.0	1.0	B	850	7d
28-73	.25	0.75	1.0	100	750	7d
29-73	.25	0.50	1.0	100	750	7d
11-72	.25	0.25	1.0	100	749	6d
143-70	.25	0.0	1.0	100	770	13d
4-72	.375	0.0	1.0	100	746	10d
224-69	.50	1.0	2.0	B	700	22d
153-70	.50	0.78	1.0	100	766	13d
12-72	.50	0.75	1.0	100	749	6d
13-72	.50	0.50	1.0	100	748	6d
193-70	.50	0.44	1.0	100	775	10d
152-70	.50	0.28	1.0	100	766	13d
14.72	.50	0.25	1.0	100	748	6d
38.73	.50	0.0	1.0	100	750	7d
6.72	.625	0.0	1.0	100	751	9d
170-70	.625	1.0	1.0	B	850	17d
15-72	.75	0.75	1.0	100	748	6d
16-72	.75	0.50	1.0	98	752	7d
17-72	.75	0.25	1.0	98	752	7d
7-72	.75	0.0	1.0	100	746	8d

*, **: z and $\frac{x}{x+y}$ refer to the biotite formula $K(Mg_xFe_yAl_z)Al_{1+z}Si_{3-z}O_{10}(OH)_2$, where $z = 3 - x - y$

***: B = run buffered by Stellite bomb; P_{H_2}, ± 5 bars; T, ± 5°C; P_{total}, ± 50 bars.

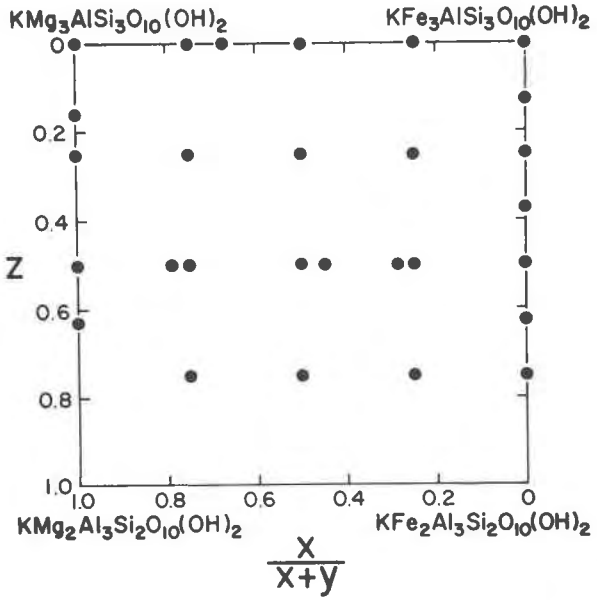

FIG. 1. Mica compositions synthesized from oxide mixes in the system Phlogopite–Annite–Aluminous-eastonite–Aluminous-siderophyllite. x, y, and z are the subscripts in the biotite formula $K(Mg_xFe_yAl_z)Al_{1+z}Si_{3-z}O_{10}(OH)_2$ where $z = 3-x-y$.

dications of oxidation was not used for the determination of physical properties.

Powder diffraction methods were used to determine unit cell parameters for all biotites in the study. The synthetic material was mixed with a CaF_2 internal standard (Baker Lot 91548; a = 5.4628(5)Å) and run at 1/4°2θ per minute through at least two complete oscillations (4 scans) from 20° to 60°2θ using Cu$K\alpha$ radiation on either a Norelco (with monochromator) or a Picker powder diffractometer (with a Ni-filter). The patterns were measured at peak top, assuming Cu$K\alpha_1$ radiation, and the average peak positions were calculated. The peaks were indexed, assuming a 1M polytype ($C2/m$). Because the relative peak positions and peak intensities vary as a function of composition, the number of reflections usable in any one refinement varied from 9–17 for the different biotites synthesized. Reflections used during the course of the study include *020, 110, 111, $\bar{1}12$, 022, 003, $\bar{1}13$, 023, $\bar{1}31$–200, 004, $\bar{1}32$–201, 132–$\bar{2}03$, $\bar{2}21$, $\bar{1}33$–202, 005, 133,* and *$\bar{3}31$–060.* Cell parameters listed in Table 2 were refined from these data, using the LSUCR program of Appleman and Evans (1973).

TABLE 2. Unit Cell and Optical Parameters for Synthetic Biotites

Run #	z	$\frac{x}{x+y}$	a(Å)	b(Å)	c(Å)	β°	V(Å^3)	Calc. $d_{\bar{3}31}$	n_γ	SEUWO*
196-70	0.0	1.0	5.317(1)	9.203(2)	10.310(2)	99.92(1)	496.9(1)	1.5345	1.583±.002	.010
222-69	0.0	1.0	5.318(2)	9.206(5)	10.308(2)	99.83(2)	497.2(3)	1.5349	1.583±.002	.016
45-73	0.0	0.75	5.337(1)	9.243(2)	10.308(2)	99.93(1)	500.9(1)	1.5406	1.608±.005	.012
40-73	0.0	0.67	5.346(2)	9.253(3)	10.314(2)	99.99(2)	502.4(2)	1.5429	1.618±.005	.015
53-73	0.0	0.50	5.361(2)	9.280(3)	10.316(2)	99.97(2)	505.4(2)	1.5473	1.635±.002	.015
68-73	0.0	0.25	5.383(1)	9.312(2)	10.324(2)	100.00(1)	509.6(1)	1.5534	1.660±.002	.010
142-70	0.0	0.0	5.404(1)	9.352(2)	10.331(2)	100.13(1)	514.0(1)	1.5596	1.687±.002	.008
67-73	0.125	0.0	5.399(1)	9.339(3)	10.329(2)	100.10(2)	512.7(1)	1.5580	1.680±.004	.013
55-73	0.167	1.0	5.311(1)	9.193(3)	10.309(2)	99.91(1)	495.8(1)	1.5329	1.584±.003	.012
189-70	0.25	1.0	5.305(1)	9.191(1)	10.305(1)	99.88(1)	495.0(1)	1.5315	1.585±.002	.006
28-73	0.25	0.75	5.330(1)	9.230(3)	10.300(2)	99.93(2)	499.1(1)	1.5386	1.607±.004	.013
29-73	0.25	0.50	5.353(1)	9.267(2)	10.303(2)	100.02(1)	503.3(1)	1.5452	1.632±.002	.012
11-72	0.25	0.25	5.373(1)	9.301(1)	10.305(1)	100.04(1)	507.1(1)	1.5508	1.656±.003	.006
143-70	0.25	0.0	5.394(1)	9.336(2)	10.300(2)	100.12(2)	510.7(1)	1.5569	1.682±.002	.010
4-72	0.375	0.0	5.385(1)	9.325(3)	10.298(2)	100.10(2)	509.1(1)	1.5543	1.673±.002	.012
224-69	0.50	1.0	5.298(0)	9.170(1)	10.304(1)	99.87(1)	493.1(1)	1.5291	1.587±.002	.003
153-70	0.50	0.78	5.318(1)	9.201(1)	10.293(1)	99.94(1)	496.1(1)	1.5347	1.606±.002	.004
12-72	0.50	0.75	5.320(1)	9.207(2)	10.298(2)	99.97(1)	496.8(1)	1.5354	1.608±.002	.010
13-72	0.50	0.50	5.341(1)	9.240(2)	10.290(1)	100.00(1)	500.1(1)	1.5414	1.629±.003	.010
193-70	0.50	0.44	5.345(1)	9.251(2)	10.277(1)	99.98(1)	500.4(1)	1.5426	1.636±.002	.007
152-70	0.50	0.28	5.358(1)	9.271(1)	10.280(1)	100.10(1)	502.8(1)	1.5463	1.647±.002	.005
14-72	0.50	0.25	5.356(3)	9.279(2)	10.285(2)	100.07(1)	503.3(2)	1.5461	1.652±.002	.011
38-73	0.50	0.0	5.374(4)	9.312(3)	10.285(2)	100.11(3)	506.7(2)	1.5514	1.673±.003	.011
6-72	0.625	0.0	5.372(2)	9.295(3)	10.277(2)	100.12(2)	505.2(1)	1.5505	1.666±.002	.013
170-70	0.625	1.0	5.293(1)	9.164(2)	10.306(1)	99.87(1)	492.5(1)	1.5278	1.588±.002	.010
15-72	0.75	0.75	5.312(1)	9.190(3)	10.297(2)	99.95(2)	495.1(1)	1.5330	1.605±.003	.013
16-72	0.75	0.50	5.325(4)	9.225(3)	10.283(2)	100.05(1)	497.4(2)	1.5373	1.628±.003	.013
17-72	0.75	0.25	5.324(4)	9.261(3)	10.274(2)	100.10(2)	500.4(3)	1.5424	1.646±.003	.014
7-72	0.75	0.0	5.366(1)	9.287(2)	10.265(2)	100.03(1)	503.7(1)	1.5488	1.664±.003	.010

* SEUWO: Standard error of a 2θ measurement of unit weight

TABLE 3. Regression Coefficients for Synthetic Biotites, Using the Regression Formula

$$g(x, y, z) = g_0 + g_1 \frac{x}{x + y} + g_2 z + g_3 \frac{zx}{x + y}$$

g(x,y,z)		g_0	$-g_1$	$-g_2$	g_3	C*	SE**	SE/Total Variation
a_o	All Biotites	5.406(1)	0.089(2)	0.056(3)	0.022(4)	.998	.002	.018
	x = 0	5.405	--	0.0531	--	.99	.002	
	y = 0	5.317	--	0.0383	--	.99	.001	
	z = 0	5.404	0.0877	--	--	.9996	.0009	
	z = .5	5.377	0.0763	--	--	.996	.002	
b_o	All Biotites	9.353(2)	0.148(3)	0.084(4)	0.019(6)	.998	.003	.016
	x = 0	9.356	--	0.0907	--	.99	.003	
	y = 0	9.205	--	0.0662	--	.995	.002	
	z = 0	9.351	0.1461	--	--	.9996	.002	
	z = .5	9.313	0.1425	--	--	.9996	.001	
c_o	All Biotites	10.329(3)	0.023(5)	0.090(6)	0.084(10)	.95	.006	.090
	x = 0	10.332	--	0.091	--	.98	.005	
	y = 0	10.309	--	0.007	--	.75	.001	
	z = 0	10.329	0.022	--	--	.96	.002	
	z = .5	10.278	0.022	--	--	.79	.005	
β	All Biotites	100.11	0.221	--	--	.93	.03	.100
	x = 0	100.13	--	0.077	--	.62	.02	
	y = 0	99.88	--	0.019	--	.15	.03	
	z = 0	100.10	0.223	--	--	.91	.04	
	z = .5	100.13	0.242	--	--	.95	.02	
V	All Biotites	514.2(2)	17.3(2)	14.3(3)	7.3(6)	.999	.3	.014
	x = 0	514.2	--	14.3	--	.998	.2	
	y = 0	497.0	--	7.5	--	.997	.1	
	z = 0	513.9	17.0	--	--	.9996	.2	
	z = .5	506.7	13.5	--	--	.999	.2	
$d_{\bar{3}31\ calc}$	All Biotites	1.5601(3)	0.0255(4)	0.0155(6)	0.0053(10)	.999	.0005	.016
	x = 0	1.5599	--	0.0151	--	.99	.0005	
	y = 0	1.5346	--	0.0111	--	.997	.0002	
	z = 0	1.5596	0.0250	--	--	.9998	.0002	
	z = .5	1.5521	0.0223	--	--	.998	.0005	
n_γ	All Biotites	1.686(1)	0.103(1)	0.029(2)	0.037(3)	.999	.001	.010
	x = 0	1.686	--	0.031	--	.95	.002	
	y = 0	1.583	--	0.008	--	.998	.001	
	z = 0	1.687	0.104	--	--	.999	.0006	
	z = .5	1.673	0.086	--	--	.9995	.0008	

* Correlation Coefficient
** Standard Error

Overlapping peaks were only used in the refinements when the intensities of those peaks, as calculated by Borg and Smith (1969) for phlogopite and fluorophlogopite, were different by at least a factor of two. The peak was then indexed as the most intense reflection. In order to test this procedure, additional refinements were performed indexing overlapping peaks as the two possible reflections and weighting these reflections according to their calculated intensities (Borg and Smith, 1969). There were no significant differences between these refinements and those presented in Table 2.

The index of refraction n_γ was measured at 25°C for each biotite, using sodium light (λ = 589nm). These data are included in Table 2.

Results

Simple linear regressions on the physical properties were calculated for four subsystems of the general biotite system, $K(Mg_xFe_y^{2+}Al_z)Al_{1+z}Si_{3-z}O_{10}(OH)_2$. Comparison of the regression coefficients (Table 3) for the subsystems $x = 0$, $y = 0$, $z = 0$, and $z = 0.5$ shows that the coefficients in the simple regressions are dependent on composition. The assumption that this variation is a linear function of composition leads to a regression equation of the form

$$g(x, y, z) = g_0 + g_1 \frac{x}{x + y} + g_2 z + g_3 \frac{zx}{x + y}.$$

Using this equation, regression coefficients for the

physical properties of all the synthetic biotites are given in Table 3. Terms were dropped and the regressions recalculated, using only the significant variables, whenever the *t*-value of any coefficient (value of the coefficient divided by the esd of that coefficient) was less than two.

A complete solid solution between iron and magnesium exists in all the biotities studied. The substitution of $2Al \rightleftarrows (Fe^{2+}$ or $Mg) + Si$, however, has previously been shown by Crowley and Roy (1964) and Rutherford (1973) to be limited. In this study, the maximum aluminum substitution occurred in biotites where $z = 0.75 \pm 0.1$.

Discussion

Variation in Cell Parameters

Considering the differences in ionic radii for the ions Mg^{2+}, Fe^{2+}, Al^{3+}, Si^{4+}, it is expected that: (1) the tetrahedral substitution of Al^{3+} for Si^{4+} will increase the dimensions of the tetrahedral sheet in the micas; (2) the octahedral substitution of Al^{3+} for Mg^{2+} or Fe^{2+} will decrease the size of the octahedral sheet; (3) the octahedral substitution of Fe^{2+} for Mg^{2+} will increase the size of the octahedral sheet. The regression equations in Table 3 show that the substitution of $Fe^{2+} \rightleftarrows Mg^{2+}$ accounts for most of the variation in cell parameters in the synthetic micas. Variations due to changes in aluminum concentration are only 25 to 50 percent as large.

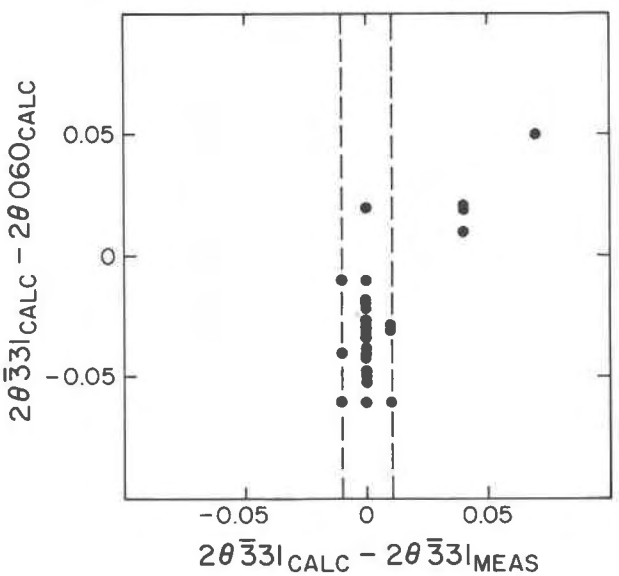

FIG. 2. A plot of the 2θ difference between $\bar{3}31$ calculated and *060* calculated, and $\bar{3}31$ calculated and $\bar{3}31$ measured for the biotites synthesized. The dashed lines indicate the estimated measuring error.

The total amount of variation in the measured physical properties ranges from 6 percent for n_γ to 0.3 percent for β. The variations in *a*, *b*, *V*, $d_{\bar{3}31}$, and n_γ are very regular and predictable if the equations in Table 3 are used. The estimated standard errors (esd's) of the regressions are all within a factor of three of the estimated standard error of the original unit cell refinement, and most are within a factor of two. The variations in *c* and β are not as regular. The esd's of the regressions for these parameters are also within a factor of three of the esd's of the cell refinements, but the total variations are much less than 1 percent, and 3 sigma represents a significant fraction (~30 percent) of the total variation.

The five parameters *a*, *b*, *V*, $d_{\bar{3}31}$, and n_γ are all excellent variables to use for the determination of compositions of the Fe-Mg-Al biotites. Practical considerations would favor the use of easily measured quantities rather than those that require a complete unit cell refinement for their determination. Only the n_γ values fit this criterion well. $d_{\bar{3}31}$ would be a good measurable quantity, except that the $\bar{3}31$ peak is interfered with by several other reflections. In particular, there is interference from the *060* peak, which has a calculated intensity approximately ½ of that of the $\bar{3}31$ peak (Borg and Smith, 1969). Furthermore, the relative calculated positions of the $\bar{3}31$ and *060* reflections vary. For most of the biotites in this study, the d_{060} was nearly equal to or slightly smaller than $d_{\bar{3}31}$. In these micas, the difference between the calculated $d_{\bar{3}31}$ and the measured $d_{\bar{3}31}$ was small and well within the error of measurement (Fig. 2). However, in four of the five biotites where the calculated d_{060} was greater than the calculated $d_{\bar{3}31}$, the differences between the calculated $d_{\bar{3}31}$ and the measured $d_{\bar{3}31}$ were significantly greater than a reasonable measuring error. Because of this uncertainty, it is felt that the measured $d_{\bar{3}31}$ and d_{060} are not reliable variables for the precise determination of biotite compositions. The calculated $d_{\bar{3}31}$ value is a very reliable composition indicator, but as with *a*, *b*, and *V*, the unit cell refinement must be carried out for its determination. Figure 3 shows one determinative plot for the biotites, using n_γ and calculated $d_{\bar{3}31}$ as the variables.

Limit of Aluminum Substitution in Biotites

Crowley and Roy (1964) reported the most aluminous composition possible for the Mg-Al biotites to be $KMg_2AlAl_2Si_2O_{10}(OH)_2$. Apparently, they were not able to obtain a 100 percent synthesis of this phase, but they were able to detect a shift in

the measured $d_{060,33l}$ in runs having this initial bulk chemistry compared with less aluminous starting compositions. Rutherford (1973) reported that he was never able to achieve greater than 80 percent synthesis of mica in runs having the bulk composition corresponding to $KFe^{2+}{}_2AlAl_2Si_2O_{10}(OH)_2$. The most aluminous Fe-biotite that he was able to synthesize was $KFe_{2.25}Al_{0.75}Al_{1.75}Si_{2.25}O_{10}(OH)_2$. Neither of these papers explained this limitation of Al substitution, except for noting that if the tetrahedral Al/Si ratio exceeds one (aluminous eastonite and aluminous siderophyllite), Al–O–Al bonds must exist in the tetrahedral layer.

This investigation agrees with the data of Rutherford (1973) on the limit of Al-substitution in the Fe-Al biotites. However, the same compositional limit, $K(Fe^{2+},Mg)_{2.25}Al_{0.75}Al_{1.75}Si_{2.25}O_{10}(OH)_2$, also appears to hold for the intermediate Fe-Mg-Al biotites. The magnesian end member appears to have an even lower solubility for aluminum (z = 0.65–0.7) rather than the higher value (z = 1) reported by Crowley and Roy (1964). Runs whose bulk compositions are more aluminous than z = 0.75 in both the iron-free and iron-bearing systems, all produce significantly less than 100 percent mica. The other phases normally present in these runs include corundum, olivine, spinel, and a low index, presumably K-rich, phase. The cell dimensions of these micas are generally consistent with those of a mica more aluminous than the z = 0.75 composition. However, because of the likelihood of some dioctahedral substitution ($2Al^{3+} \rightleftarrows 3(Fe^{2+},Mg^{2+})$), it cannot be assumed that a more aluminous trioctahedral biotite has been produced.

The argument that the limit of the aluminum substitution in biotite is due to the aluminum avoidance rule is not cogent in light of the existence of the structurally similar mica xanthophyllite ($CaMg_2Al(Al_3SiO_{10})(OH)_2$) (Takeuchi and Sadanaga, 1966), which violates the rule. The existence of the dioctahedral aluminous micas, muscovite and paragonite, makes an octahedral aluminum avoidance rule even less acceptable. A more plausible explanation can be based on a consideration of a limiting size for the interlayer site.

In the mica structure, the dimensional misfit between the octahedral layer and the tetrahedral layers can be compensated for in two ways. There can be flattening of the octahedra to enlarge the octahedral sheet, or a rotation of the tetrahedra to make the tetrahedral sheet smaller. The tetrahedra can rotate from a perfect hexagonal array (α-rotation = 0°) towards a close-packed array (α-rotation = 30°) (Donnay, Donnay, and Takeda, 1964). Coincident with this rotation, the interlayer site changes from a regular 12-coordinated site (when α = 0°) to a regular 6-coordinated site when α = 30°. Assuming that the basal layer of oxygens in the tetrahedral sheets remains co-planar, Donnay, Donnay, and Takeda (1964) calculated and plotted the relations between α-rotation, b, and the mean K–O bond length. These calculated values of α and K–O bond lengths for the biotite sub-series x = 0, y = 0, z =0.5, and z = 0 are given in Table 4. The α-rotation and K–O bond lengths in the most aluminous biotites range from 12° and 2.89Å for the magnesium-free system to 14.7° and 2.77Å for the iron-free system. The lower limits of the observed range of K–O bond lengths for potassium in 6- to 12-fold coordination *(International Tables)* indicate that K–O bond lengths less than ~2.8Å would be relatively unstable. Although precise comparisons among the synthetic biotites cannot be expected because of the simplified model used in the calculation of the bond lengths, the predicted short K–O bond lengths for the most aluminous biotites strongly suggest that the size of the interlayer cation controls the maximum amount of tetrahedral rotation that can occur in a stable mica. A limit on the amount of tetrahedral rotation is tantamount to a limit on the amount of aluminum substitution in the trioctahedral biotites, because additional substitution of tetrahedral and octahedral aluminum enlarges the misfit between the octahedral

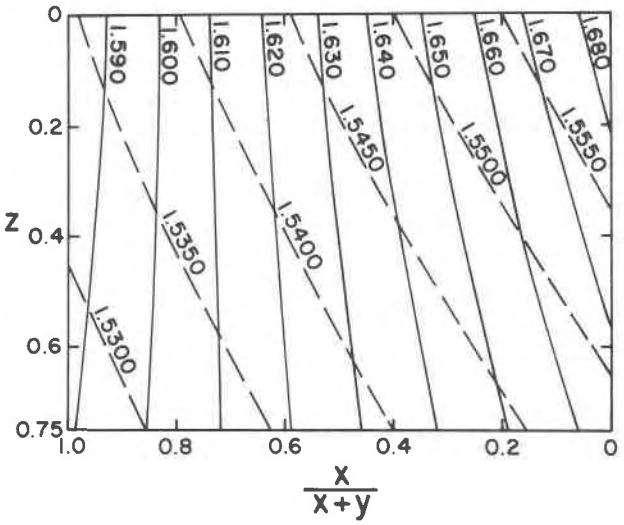

FIG. 3. Determinative plot for the Fe-Mg-Al biotites using n_γ (solid lines) and calculated $d_{\bar{3}b1}$ (dashed lines) as variables. The x, y, and z are the subscripts in the biotite formula $K(Mg_xFe_yAl_z)Al_{1+z}Si_{3-z}O_{10}(OH)_2$, where $z = 3-x-y$.

TABLE 4. Calculated Tetrahedral Rotations, Octahedral Flattening, and K–O Bond Lengths for Ideal Trioctahedral Biotites

$\frac{x}{x+y}$	z	b_o calc	<dt>*	<do>**	α***	ψ$^{\Delta}$	K–O$^{\Delta\Delta}$
1.0	0.0	9.205Å	1.649Å	2.06Å	9.3°	59.3°	2.92Å
1.0	0.25	9.189	1.659	2.04	11.7°	60.1°	2.85
1.0	0.50	9.173	1.669	2.03	13.7°	60.4°	2.79
1.0	0.65	9.163	1.675	2.02	14.7°	61.3°	2.77
0.5	0.0	9.279	1.649	2.09	5.9°	58.7°	3.02
0.5	0.25	9.260	1.659	2.07	9.4°	59.4°	2.95
0.5	0.50	9.242	1.669	2.06	11.8°	59.7°	2.88
0.5	0.75	9.223	1.679	2.03	13.8°	61.0°	2.82
0.0	0.0	9.353	1.649	2.11	∿0.0°	58.5°	3.16
0.0	0.25	9.332	1.659	2.10	6.0°	58.8°	3.07
0.0	0.50	9.311	1.669	2.08	9.5°	59.5°	2.98
0.0	0.75	9.290	1.679	2.06	12.0°	60.2°	2.89

* Average <T-O> bond length calculated from Hazen and Burnham (1973)

** Average <M-O> bond length estimated using O^{-2} = 1.34, Mg^{+2} = .72, Al^{+3} = .53, Fe^{+2} = .78 {Shannon and Prewitt (1970); Hazen and Burnham (1973)}

*** – Calculated from $\cos\alpha = \frac{b_{obs}}{4\sqrt{2}\ \langle dt\rangle}$

Δ – Calculated from $\sin\psi = \frac{b_{obs}}{3\sqrt{3}\ \langle do\rangle}$

$\Delta\Delta$ – Donnay, Donnay, and Takeda (1964)

and tetrahedral sheets and thereby increases the amount of necessary tetrahedral rotation.

The brittle micas margarite and xanthophyllite, which have more aluminum in the tetrahedral sites and greater α-rotations than the biotites, have the smaller Ca^{2+} atom in the interlayer site. The observed tetrahedral rotations in the dioctahedral micas muscovite (α = 12.8°) (Radoslovich, 1960) and paragonite (α = 15.9°) (Burnham and Radoslovich, 1964) also indicate that the size of the interlayer cation in part controls the amount of tetrahedral rotation that occurs in the mica structure.

If the interlayer site controls the maximum value of α and thus the maximum amount of Al-substitution, it should be possible to synthesize a more Al-rich biotite if a smaller interlayer cation is substituted at the same time. In order to test this hypothesis, a trioctahedral mica having the composition $NaMg_2AlAl_2Si_2O_{10}(OH)_2$ was synthesized from an oxide mix held at 600°C and 4000 bars water pressure for 7 days. The mica is similar to the Na-phlogopite synthesized by Carman (1974) in that it was reversibly hydrated to 12 and 15Å mica phases. Cell dimensions were determined for the 10Å phase on the basis of the 1*M* polytype used for the other biotites reported. These data are shown in Table 5. Compared with the unit cell dimensions for the most aluminous K-Mg-Al biotite synthesized, the significant reduction in the *a* and *b* dimensions at the same time that the average *T*–O bond length increases can only be accounted for by a greater α-rotation in the Na-mica. The value calculated, again assuming that the basal oxygens are coplanar, is 18.8°. An extrapolation of Donnay, Donnay, and Takeda's (1964) calculations yields an Na–O bond length of 2.6Å. This compares well with the Na–O bond length of 2.64Å observed in paragonite (Burnham and Radoslovich, 1964).

Polytypism

The cell dimensions for all biotites synthesized in this study were refined assuming a 1*M* polytype (*C*2/*m*). Many of the data were also refined assuming a 3*T* polytype, but overall the esd's were slightly smaller for the 1*M* refinements. Detailed crystal-structure refinements of several natural and synthetic biotites have shown the common occurrence of the 1*M* polytype (Steinfink, 1962; McCauley, Newnham, and Gibbs, 1973; Hazen and Burnham, 1973; Donnay, Morimoto, Takeda, and Donnay, 1964; Teipkin, Drits, and Alexandrova, 1969; Zvyagin and Mishchenko, 1962). Although 1*M* and 3*T* biotites cannot be reliably differentiated by using powder X-ray techniques, and the polytypism of several natural biotites has been shown to be complex (Ross, Takeda and Wones, 1966; G. V. Gibbs and J. Leiss, personal communication, 1974), the authors feel justified in presenting the data in a 1*M* format. In this way, the results are most consistent with our observations, and the data are directly comparable with the published data of previous workers (Wones, 1963; Crowley and Roy, 1964; Rutherford, 1973). No additional peaks indicating other possible polytypes showed up in any of the high-temperature runs (≥700°C) of this investigation.

In the early part of the study, some syntheses were performed at lower temperatures (500°–600°C). Although the maxima in the powder-diffraction patterns were not sharp for these micas, 5–8 broad peaks

TABLE 5. Comparison of the Unit Cell Parameters for Na-Aluminous Eastonite and the K-Mica $KMg_{2.38}Al_{0.62}Al_{1.62}Si_{2.38}O_{10}(OH)_2$

	$NaMg_2AlAl_2Si_2O_{10}(OH)_2$	$KMg_{2.38}Al_{.62}Al_{1.62}Si_{2.38}O_{10}(OH)_2$
a(Å)	5.216(3)	5.293(1)
b(Å)	9.046(2)	9.164(2)
c(Å)	9.807(3)	10.306(1)
β (deg)	100.20 (3)	99.87 (1)
V(Å^3)	455.5 (2)	492.5 (1)
α*(deg)	18.8	14.7
Na–O**(Å)	2.6	
K–O**(Å)		2.77

* Calculated from $\cos\alpha = \frac{b_{obs}}{4\sqrt{2}\langle dt\rangle}$

** Estimated from Donnay, Donnay, and Takeda (1964)

appearing in some of the patterns could not be accounted for in a $1M$ mica model or as any likely additional phase. It was discovered that the powder patterns could be greatly improved if after crystallization at ~600°C and 1–2 kbar for 7 days the temperature was raised to ~800°C for another 4–7 days. When this was done, the broad peaks on the 600°C material became sharp, well-defined reflections having no apparent loss in intensity or shift in position.

Unit cell refinements of these peaks along with three ($00l$) peaks are consistent with those of a $2M_1$ mica. Apparently these low-temperature runs produce either a mixture of $2M_1$ and $1M$ or $3T$ mica polytypes or some other more complex polytype. Many experiments were initiated in order to synthesize a pure $2M_1$ biotite. Temperature, pressure, composition, and run duration were all varied, with little success. Attempts to change a $1M$–$2M_1$ mixture to a pure $1M$ phase were also unsuccessful.

Although a 100 percent synthesis of $2M_1$ mica was never achieved, the yield did vary for the different compositions and conditions used. Maximum synthesis is estimated to be in the range of 20–50 percent. The following factors affected the yield of the $2M_1$ polytype:

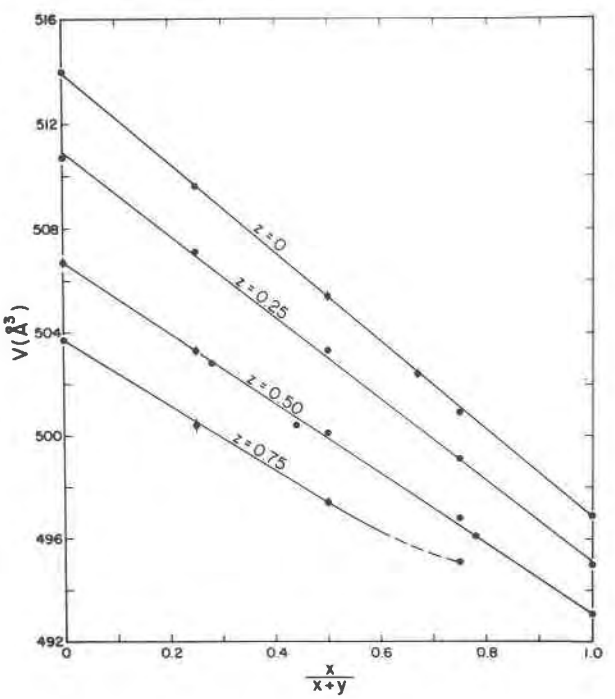

FIG. 4. Plot of unit cell volume versus $\frac{x}{x+y}\left(=\frac{\text{Mg}}{\text{Mg}+\text{Fe}}\right)$ at constant aluminum content (z).

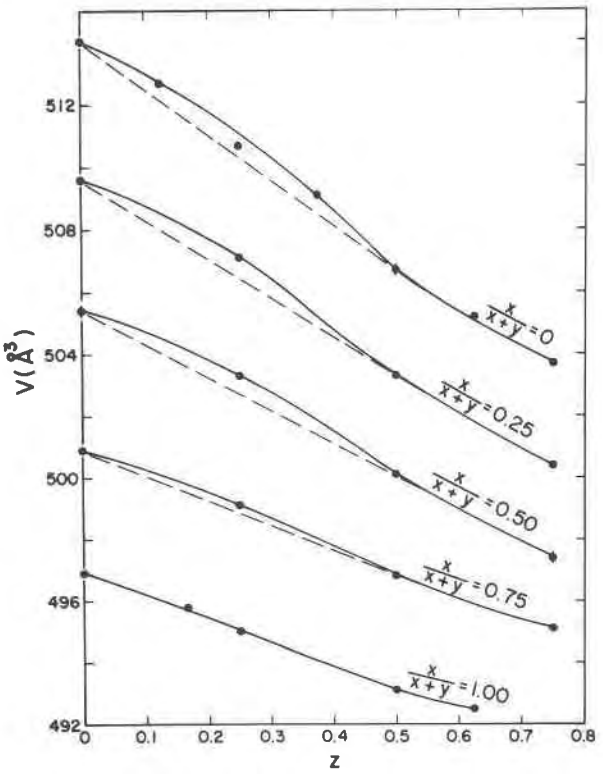

FIG. 5. Plot of unit cell volume versus z (octahedral-Al) at constant $\frac{x}{x+y}\left(=\frac{\text{Mg}}{\text{Mg}+\text{Fe}}\right)$.

1. Temperature: the best yield occurred when temperatures of ~600°C were followed by ~800°C; in runs at $T<600$°C, the yields were no greater, and in runs initially at 650°C, the yields were lower; initial runs at $T\geq 700$°C yielded no $2M_1$ mica.
2. Composition: the $2M_1$ phase grew best in the Mg-biotites in which the octahedral Al content was less than 1/6 of the total octahedral occupancy ($z<0.5$); the $2M_1$ phase did not develop well in any of the Fe-rich biotites.

The relative stability of the $1M$ and $2M_1$ polytypes remains unknown. Solely on the basis of the synthesis data presented here, we suggest that the $2M_1$ phase is more stable at lower temperatures than the $1M$ phase. This agrees with the conclusions presented by Yoder and Eugster (1954). However, the very small free-energy difference anticipated between these two polytypes suggests that neither an attempt at a more accurate determination of the stability nor the application of this crude relationship to natural systems would be successful or of meaningful value.

Solution Properties

Experimental data reported by Wones, Burns, and Carroll (1971) and Wones (1972) indicate that the phlogopite-annite solid solution is essentially ideal. Because one of the octahedral sites in the mica structure is smaller than the other two, it might be expected that, as the size contrast increases between the octahedral cations, octahedral ordering would occur in the biotites as it does in the dioctahedral micas margarite and muscovite and in the trioctahedral mica xanthophyllite. One indication of this nonideality appears when plots of unit cell volume versus the octahedral aluminum content at constant $\frac{Mg}{Mg+Fe}$ (Fig. 5) are compared with the plots of unit cell volume versus the $\frac{Mg}{Mg+Fe}$ ratio at constant values of octahedral aluminum (Fig. 4). The data in Figure 4 show that the volume of mixing is approximately zero for $Fe^{2+} \rightleftarrows Mg^{2+}$ substitution in micas of constant aluminum concentration and is therefore consistent with the ideal solution model. Figure 5 shows that the volume of mixing for the substitution $(Fe^{2+},Mg^{2+})^{VI} + Si^{IV} \rightleftarrows Al^{VI} + Al^{IV}$ varies from approximately zero for the Mg-biotites to more and more positive values as the amount of Fe^{2+} is increased. Experimental work on the determination of the activity of the annite component in the Fe-Al biotites is presently in progress to confirm this nonideal solution behavior.

Acknowledgments

The authors would like to thank Drs. E-an Zen and Malcolm Ross of the United States Geological Survey for their helpful reviews of the manuscript. The research was supported at M.I.T. by NSF Grants GA1109 & GA13092 and at VPISU by NSF Grant GA-32267.

References

Appleman, D. E., and H. T. Evans (1973) Job 9214: Indexing and least-squares refinement of powder diffraction data. *U.S. Dept. Commerce, Natl. Tech. Inform. Serv.* **PB 216 188.**

Borg, I. Y., and K. K. Smith (1969) Calculated X-ray powder patterns for silicate minerals. *Geol. Soc. Am. Mem.* **122,** 896.

Burnham, C., and E. W. Radoslovich (1964) Crystal structures of coexisting muscovite and paragonite. *Carnegie Inst. Wash. Year Book,* **63,** 232–236.

Carman, J. H. (1974) Synthetic sodium phlogopite and its two hydrates: stabilities, properties, and mineralogic implications. *Am. Mineral.* **59,** 261–273.

Crowley, M. S., and Rustum Roy (1964) Crystalline solubility in the muscovite and phlogopite groups. *Am. Mineral.* **49,** 348–362.

Donnay, G., J. D. H. Donnay, and H. Takeda (1964) Trioctahedral one-layer micas. II. Prediction of the structure from composition and cell dimensions. *Acta Crystallogr.* **17,** 1374–1381.

———, N. Morimoto, H. Takeda, and J. D. H. Donnay (1964) Trioctahedral one-layer micas. I. Crystal structure of a synthetic iron mica. *Acta Crystallogr.* **17,** 1369–1373.

Eugster, H. P., A. L. Albee, A. E. Bence, J. B. Thompson, Jr., and D. R. Waldbaum (1972) The two-phase region and excess mixing properties of paragonite-muscovite crystalline solutions. *J. Petrol.* **13,** 147–179.

Hazen, R. M., and C. W. Burnham (1973) The crystal structures of one-layer phlogopite and annite. *Am. Mineral* **58,** 889–900.

———, and D. R. Wones (1972) The effect of cation substitutions on the physical properties of trioctahedral micas. *Am. Mineral.* **57,** 103–125.

McCauley, J. W., R. E. Newnham, and G. V. Gibbs (1973) Crystal structure analysis of synthetic fluorophlogopite. *Am. Mineral.* **58,** 249–254.

Radoslovich, E. W. (1960) The structure of muscovite, $KAl_2(AlSi_3)O_{10}(OH)_2$. *Acta Crystallogr.* **13,** 919–932.

Radoslovich, E. W. (1963) The cell dimensions and symmetry of layer-lattice silicates. IV. Interatomic forces. *Am. Mineral.* **48,** 76–99.

Ross, M., H. Takeda, and D. R. Wones (1966) Mica polytypes: systematic description and identification. *Science,* **151,** 191–193.

Rutherford, Malcolm J. (1973) The phase relations of aluminous iron biotites in the system $KAlSi_3O_8$–$KAlSiO_4$–Al_2O_3–Fe–O–H. *J. Petrol.* **14,** 159–180.

Schairer, J. F., and N. L. Bowen (1955) The system K_2O–Al_2O_3–SiO_2. *Am. J. Sci.* **253,** 681–746.

Shannon, R. D., and C. T. Prewitt (1970) Revised values of effective ionic radii. *Acta Crystallogr.* **B26,** 1046–1048.

Shaw, H. R. (1963) Hydrogen-water, vapor mixtures: Control of hydrothermal atmospheres by hydrogen osmosis. *Science,* **139,** 1220–1222.

Steinfink, H. (1962) Crystal structure of a trioctahedral mica: phlogopite. *Am. Mineral.* **47,** 886–896.

Takeuchi, Y., and R. Sadanaga (1966) The crystal structure of xanthophyllite revised. *Mineral. J.* **4,** 421–437.

Teipkin, E. V., V. A. Drits, and V. A. Alexandrova (1969) Crystal structure of iron biotite and construction of several structural models for trioctahedral micas. *Int. Clay Conf. Proc.* **1,** Tokyo.

Wones, D. R. (1963) Physical properties of synthetic biotites on the join phlogopite-annite. *Am. Mineral.* **48,** 1300–1321.

——— (1972) Stability of biotite: A reply. *Am. Mineral.* **57,** 316–317.

———, R. G. Burns, and B. M. Carroll (1971) Stability and properties of synthetic annite (abstr.). *Trans. Am. Geophys. Union,* **52,** 369.

Yoder, H. S., Jr., and H. P. Eugster (1954) Phlogopite synthesis and stability range. *Geochim. Cosmochim. Acta,* **6,** 157–185.

Zvyagin, B. B., and K. S. Mishchenko (1962) Electronographic data on the structure of phlogopite-biotite. *Sov. Phys. Crystallogr.* **7,** 502–505.

Manuscript received, January 31, 1975; accepted for publication, May 2, 1975.